Pinch-off singularities in rotating Hele-Shaw flows at high viscosity contrast

E. Alvarez-Lacalle,[1] J. Casademunt,[2] and J. Eggers[3]
[1]*Departament de Física Aplicada, Universitat Politècnica de Catalunya, Av. Dr. Marañon 50 (EPSEB), E-08028 Barcelona, Spain*
[2]*Departament d'ECM, Universitat de Barcelona, Av. Diagonal 647, E-08028 Barcelona, Spain*
[3]*School of Mathematics, University of Bristol, University Walk, Bristol BS8 1TW, United Kingdom*
(Received 17 February 2009; revised manuscript received 4 September 2009; published 16 November 2009)

We study the evolution of a family of dumbbell-shaped liquid patches surrounded by air inside a rotating Hele-Shaw cell with lubrication methods and numerical simulations. Depending on initial conditions, the dumbbell either stretches to infinity, pinches off at the neck to form a droplet, or collects into a circular drop at the center of rotation. Whether or not pinch-off occurs results from a subtle interplay between centrifugal and capillary forces. In particular, rotation may delay or even prevent pinch-off from occurring owing to stretching and smoothing of the fluid neck. However, frequently rotation may have the opposite effect leading to pinch-off where the relaxation toward a circular drop would be observed in an ordinary Hele-Shaw cell.

DOI: 10.1103/PhysRevE.80.056306 PACS number(s): 47.55.D−, 68.03.Cd, 47.20.Ma, 47.11.−j

I. INTRODUCTION

Topological singularities and, in particular, interface pinch-off of two-phase fluid flows have been the object of intense study in the last decades [1–4]. Hydrodynamics alone has been shown to be sufficient to account for the existence of finite-time pinch-off singularities, starting from regular initial conditions. In fact, when two interfaces approach each other the continuum hydrodynamic description must eventually fail close to the interface contact. However, it has been shown that the Navier-Stokes equations can be continued uniquely through the singularity [1]. Thus, the molecular effects that eventually regularize the singularity and implement the interface reconnection act instantaneously in the macroscopic scale.

In a Hele-Shaw cell with a gap spacing b, the interface dynamics defines a well-known two-dimensional (2D) free-boundary problem [5–7]. When the cell is rotating with an angular velocity Ω (see Fig. 1), the equation of motion of a liquid with viscosity μ, density ρ, and surface tension σ surrounded by air is described by the in-plane velocity $\vec{v}=-b^2/(12\mu_i)(\vec{\nabla}p_i-\rho_i\Omega^2 r\hat{r})$, together with the two boundary conditions at the interface, the Young-Laplace pressure drop $p_2-p_1=\sigma\kappa$ (where κ is the in-place curvature) and the continuity of normal velocity $v_{n1}=v_{n2}$ [8–10]. In the absence of rotation it has been shown that the two-dimensional dynamics can lead to finite-time pinch-off [11–16]. In a specific class of initial conditions that is directly relevant to the present study, surface tension alone has been shown to drive two droplets of fluid connected by a neck to finite-time pinch-off in two-dimensional simulations [17,18]. Rotation introduces the additional feature of spontaneously generating long and thin (radial) filaments with droplet-shaped ends as the natural evolution of an initial interface close to circular, where the more dense fluid is inside. Experiments in rotating Hele-Shaw cells [19,20] have shown that when the interface separates two liquids the droplets do pinch off rather often, while this process is rare when one liquid is surrounded by air (high viscosity contrast).

Although it may not be simple to elucidate whether singularities are inherent to the 2D Hele-Shaw dynamics, or associated to three-dimensional effects, this question is particularly relevant in this problem since, in principle, the 2D effective description ceases to be valid at the relatively large scale b. In an accompanying paper [21], the question of the relevance of singularities in the 2D Hele-Shaw equations to experiments in actual Hele-Shaw cells has been addressed in detail. Reference [21] is complementary to the work reported here in both methods and focus. There, a phase-field (diffuse-interface) approach is used to study the occurrence of finite-time pinch-off and its dependence on viscosity contrast. This aspect would be very involved by means of sharp-interface methods but is particularly suitable to phase-field methods. The main conclusion of [21] is that pinch-off singularities typically exist in rotating Hele-Shaw flows for low viscosity contrast, in a regime where centrifugal forces dominate over capillary forces, and are inherent to the 2D dynamics. In the high viscosity contrast limit, however, the phase-field ap-

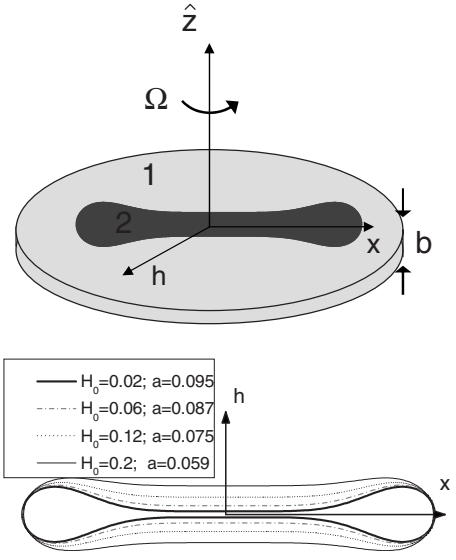

FIG. 1. Top: sketch of a top-side view of the radial Hele-Shaw cell with rotation where the inner fluid (named fluid 2) and the outer fluid (named fluid 1) are indicated with different gray levels. At the bottom, a top view of the cell with characteristic initial condition with dumbbell shapes.

proach is not conclusive. Instead, a more traditional sharp-interface formulation based on a lubrication analysis seems adequate and powerful at high viscosity contrast. This is precisely the aim of the present paper.

The outline of this paper is as follows. First, we recall the set of equations that drive the rotational Hele-Shaw cell and perform a lubrication analysis. The resulting lubrication equation is analyzed from the perspective of the competition between rotational and capillary effects. Within the lubrication equation the effect of rotation is typically to postpone or eliminate finite-time pinch-off. However, the matching of the lubrication region to the moving droplet at the end of the filament imposes in general nontrivial boundary conditions to the lubrication equation. We perform numerical simulations of the evolution of a uniparametric family of initial conditions that includes the droplets at the end of the filaments (dumbbell shapes). This permits us to study the existence of singularities in a well characterized problem strongly related to previous experimental results. The competition of various physical effects leads to different types of approach to pinch-off depending on whether the drop recedes toward the center or is expelled toward infinity. We demonstrate a strong influence of the boundary conditions to the lubrication equation on the dynamics of approach to pinch-off. Finally, we conclude with some remarks on how our results relate to previous experiments and hint at possible future experimental work.

II. LUBRICATION APPROXIMATION

In this section we derive the so-called lubrication approximation for the dynamics of a thin rotating filament. Our starting point is the vortex-sheet formulation of the 2D Hele-Shaw equations for an interface $\vec{r}(s,t)$ in the presence of rotation [5,9]:

$$\vec{r}(s,t)=[x(s,t),y(s,t)], \quad \frac{d\vec{r}(s,t)}{dt}\cdot\hat{n}=\vec{U}\cdot\hat{n}, \tag{1}$$

with

$$\vec{U}=\frac{1}{2\pi}P\int_0^L \frac{[y(s')-y(s),x(s)-x(s')]}{[x(s)-x(s')]^2+[y(s)-y(s')]^2}\gamma(s',t)ds', \tag{2}$$

where the integral is along the interface (L being the total length of the interface), P is the Cauchy principal part, and the vorticity is

$$\gamma=2B\kappa_s-2A(\vec{U}\cdot\hat{s})+2D\vec{r}\cdot\hat{\mathbf{s}}. \tag{3}$$

Here we use the abbreviations

$$B=\frac{b^2\sigma}{12(\mu_1+\mu_2)}, \quad D=\frac{b^2\Omega^2(\rho_2-\rho_1)}{12(\mu_1+\mu_2)} \tag{4}$$

and

$$\kappa=\frac{dx}{ds}\frac{d^2y}{ds^2}-\frac{dy}{ds}\frac{d^2x}{ds^2}, \tag{5}$$

where $A=(\mu_2-\mu_1)/(\mu_1+\mu_2)$ is the viscosity contrast and $\vec{U}$ is the mean fluid velocity at the interface.

We are interested in the dynamics of thin filaments oriented radially. In order to isolate the contributions from the lubrication region, and following the same procedure as in Ref. [16], we consider an infinitely long thin fluid filament which we assume asymmetric along the x axis and is defined by the distance to the x axis $y=h(x)$. Parametrized with x, the evolution equation for h reads

$$\partial_t h=U_{\hat{y}}-U_{\hat{x}}\partial_x h, \tag{6}$$

where $\vec{U}$ is now written as $\vec{U}(x,t)=U_{\hat{x}}\hat{x}+U_{\hat{y}}\hat{y}$, which we assume to vary only in the x direction. Therefore, we have

$$\vec{U}(x,t)=\frac{1}{2\pi}P\int_{-\infty}^{+\infty}\frac{[h(x')-h(x),x-x']}{(x-x')^2+[h(x')-h(x)]^2}\Upsilon(x')dx' - \frac{1}{2\pi}P\int_{-\infty}^{+\infty}\frac{[-h(x')-h(x),x-x']}{(x-x')^2+[h(x')+h(x)]^2}\Upsilon(x')dx', \tag{7}$$

where $\Upsilon=\gamma(1+h_x^2)$. Equation (3) reads in terms of x as

$$\Upsilon/2=B\partial_x\kappa-A\vec{U}\cdot(\hat{x}+\hat{y}\partial_x h)+D(x+h\partial_x h). \tag{8}$$

To perform a lubrication analysis we assume the interface height $h(x,t)$ to vary on a scale Δh much smaller than the scale of horizontal variations ℓ and expand formally all quantities in powers of $\varepsilon=\Delta h/\ell$ to obtain an evolution equation for h up to first order in ε.

We now scale h with Δh, x with ℓ, and the interface velocity $\vec{U}$ with $V_0=(B/\ell^2)+D\ell$. We expand any quantity Q as $Q=Q^{(0)}+\epsilon Q^{(1)}+\epsilon^2 Q^{(2)}$, so that the evolution equation for h up to $O(\varepsilon)$ becomes

$$\partial_t h=U_{\hat{y}}^{(1)}-\partial_x h U_{\hat{x}}^{(0)}+\varepsilon(U_{\hat{y}}^{(2)}-\partial_x h U_{\hat{x}}^{(1)}), \tag{9}$$

where we have anticipated that $U_{\hat{y}}^{(0)}=0$. Further, by expanding $\vec{U}$ and Υ along the same lines as in Refs. [9,16], we find [23]

$$U_{\hat{x}}^{(0)}=\frac{1}{2}\Upsilon^{(0)}, \tag{10a}$$

$$U_{\hat{x}}^{(1)}=\frac{1}{2}\Upsilon^{(1)}+H[\partial_x(h\Upsilon^{(0)})], \tag{10b}$$

$$U_{\hat{y}}^{(1)}=-\frac{1}{2}[\partial_x(h\Upsilon^{(0)})+h\partial_x\Upsilon^{(0)}], \tag{10c}$$

$$U_{\hat{y}}^{(2)}=-\frac{1}{2}[\partial_x(h\Upsilon^{(1)})+h\partial_x\Upsilon^{(1)}]-hH[\partial_x^2(h\Upsilon^{(0)})], \tag{10d}$$

$$\Upsilon^{(0)}=\frac{2LD}{(1+A)V_o}x, \tag{10e}$$

$$\Upsilon^{(1)} = \frac{2B}{(1+A)V_o L^2}\partial_x^3 h - \frac{2A}{1+A}H[\partial_x(h\Upsilon^{(0)})]. \quad (10f)$$

Here $H[f](x)=\pi^{-1}P\int_{-\infty}^{+\infty}f(x')dx'/(x-x')$ is the Hilbert transform of $f(x)$. The major difference between the weakly nonlinear expansion performed in [9] and this lubrication approximation is the appearance of the second integral in Eq. (7). Its expansion is not trivial as pointed out in [16]; there it was solved using limiting procedures, the Plemelj formula, and delta function representations.

Substituting these results into Eq. (9) and keeping the scaling of lengths to show explicitly the orders in ε, we finally obtain

$$\frac{1+A}{2}\partial_t h = -D\partial_x(xh) - \varepsilon B\partial_x(h\partial_x^3 h) - D\varepsilon\frac{(1-A)}{1+A}\partial_x(hH[\partial_x(xh)]). \quad (11)$$

This equation sets the basic framework for the discussion of pinch-off phenomena in rotating Hele-Shaw flows. Note that if the viscosity of the outer fluid is neglected ($A=1$), the equation becomes local. Herein, we will restrict to this particular case.

III. COMPETITION BETWEEN CAPILLARY AND CENTRIFUGAL FORCES

The starting point of our analysis is Eq. (11) with $A=1$, which in the original variables reads

$$\partial_t h = -D\partial_x(xh) - B\partial_x(h\partial_x^3 h). \quad (12)$$

Equation (12) has been studied extensively in the absence of rotation ($D=0$). It has been shown by Goldstein *et al.* [12,15,16] that capillary forces may lead to finite-time pinch-off for some specific boundary conditions. For the same uniparametric class of initial conditions discussed below, Almgren *et al.* [17,18] identified the regions that either evolved without singularities toward a circular droplet or developed a finite-time pinch-off. If, on the contrary, the problem is dominated by centrifugal forces ($B=0$), it is easy to show that Eq. (12) has a class of solutions of the form

$$h(x,t) = e^{-Dt}h_0(e^{-Dt}x), \quad (13)$$

where $h_0(x)$ is an arbitrary initial condition. This means that centrifugal forcing alone stretches the fluid filament as it thins, in such a way that pinch-off would ultimately occur only at infinite time.

As shown by experiments [19] and numerics [21], centrifugal forcing will tend in general to produce interface configurations with elongated thin radial filaments in the long time evolution of fingering patterns. Once these radial filaments are formed, however, the evolution toward a singularity as a result of the nonlinear capillary term will oppose the stretching effect of the centrifugal force, even though the latter produces an overall thinning of the fluid filament. The outcome of this competition between capillary and centrifugal forces is indeed nontrivial and will be discussed in detail in the following sections. Before proceeding to the full numerical study, however, it is useful to make first some approximate analytical considerations that may shed some light on the problem.

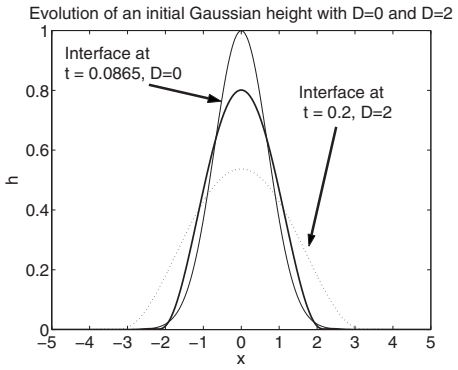

FIG. 2. Evolution of an initial Gaussian interface which is set to zero and with zero derivative in the interval ($x=\pm 5, \pm\infty$). We plot the initial condition and two evolved interfaces corresponding to the cases with rotation ($D=2$, $B=1$) and without rotation ($D=0$, $B=1$) at respective times related by scaling (14). They are taken after $t=0.2$ and $t=0.0865$, respectively. The interface obtained at $t=0.2$ with rotation is reproduced exactly by scaling the interface evolved without rotation obtained at $t=0.0865$. This scaling involves stretching and reducing the height using an exponential factor as indicated in the text.

In fact, a first insight can be gained with an appropriate change in variables of the form

$$G = he^{Dt}, \quad \eta = xe^{-Dt}, \quad \tau = \frac{B}{5D}(1-e^{-5Dt}), \quad (14)$$

which turns Eq. (11) into the form of the purely capillary case,

$$\partial_\tau G = -\partial_\eta(G\partial_\eta^3 G). \quad (15)$$

This means that, except for boundary conditions, a nonuniform scaling of time and space reduces the problem to the case without rotation. Figure 2 shows the basic effects of this scaling in the case of a localized structure, for which no significant effect of boundary conditions may be expected. We plot the evolution of an initial Gaussian interface with surface tension and rotation ($B=1$, $D=2$) after $t=0.2$ and compare it with the equivalent case without rotation ($B=1$, $D=0$) at time $\tau=[1.0-\exp(-10t)]/10=0.0865$. The two curves match exactly when the scaling that combines stretching and thinning according to Eq. (14) is applied.

Remarkably, this mapping suggests that the long time evolution of the case with rotation is related to the behavior of the case without rotation for a finite time. Indeed, the time variable τ is bounded by a maximum value $\tau_m=\frac{B}{5D}$, so that an infinite-time lapse for the physical time t is mapped into a finite-time interval for τ. Finite-time pinch-off singularities are, thus, in principle possible in the presence of rotation if they occur at finite time also in the case without rotation. However, the contrary is also possible, that is, rotation would prevent the formation of finite-time pinch-off for those situations where the pinch-off of the case without rotation occurs

too late. Specifically, in situations where Eq. (15) predicts no singularity for $\tau < \tau_m$, one should expect that there will be no singularity in the original variables at finite time for the case with rotation. Accordingly, the behavior of the physical variables will be asymptotically that of the purely rotating case [Eq. (13)]. On the other hand, if Eq. (15) predicts a finite-time singularity at $\tau_s < \tau_m$ then one may expect also a finite-time singularity in the physical time $t_s = \frac{1}{5D}\ln(1-\frac{5D\tau_s}{B})^{-1}$. The mapping of our problem to the one without rotation is obviously not exact because the boundary conditions imposed by the matching to the nonlubrication region are different in both cases. That is, in the variables where the lubrication approximation takes the form of Eq. (15) the dynamics of the droplet closing the fluid filament are different in the two problems, thus, resulting in different boundary conditions for the lubrication equation. Although inexact, the argument is useful both to intuit the connection between the two problems and as an explicit (albeit approximate) prediction of the behavior for the case of rotation.

This analysis is interesting to the extent that it yields quantitative predictions under the assumption that boundary conditions for the pinch-off regions are not relevant. For example, if τ_0 is the time at which a particular interface pinches off in the case without rotation, this approximation implies that the maximum rotation at which one would expect finite-time pinch-off is given by $D/B = 1/(5\tau_0)$. Accordingly, failure of this prediction will signal a crucial role of the effective boundary conditions for the lubrication equation due to the matching with the droplet that closes the fluid filament.

IV. MODEL EQUATION AND NUMERICAL INTEGRATION

In order to fix a representative class of initial conditions that is relevant to the present discussion, and for the sake of comparison, we choose the uniparametric family of dumbbell-shaped interfaces studied by Almgren *et al.* [17,18], which take the form

$$\theta = s + \left(\frac{2}{3} + 5a\right)\sin(2s) + \left(\frac{1}{12} + 4a\right)\sin(4s) + a\,\sin(6s) + \frac{\pi}{2}, \tag{16}$$

where s is arclength, $dh/dx = \tan\theta$, and a parametrizes the family of interface shapes. For convenience, we will parametrize the initial condition with the interface height $h(x=0,\ t=0)$ which we designate by H_0.

To resolve the pinch-off region properly, in our numerical integration we refine the mesh size in the pinching region progressively. Treating a closed interface presents a problem, since the last term of Eq. (12), which is related to the curvature of the interface, becomes infinite at the end of the finger. We deal with this problem by modifying the equation through a partial resummation of all higher-order terms involving curvature as it has been done in [22] (for further information see also [1]). In this way the problem is defined by

$$\partial_t h = -\partial_x(hu), \quad u = Dx + B\partial_x\kappa,$$
$$\partial_t l = u(l), \quad \kappa = \frac{\partial_x^2 h}{[1+(\partial_x h)^2]^{3/2}}, \tag{17}$$

where h is the height of the interface, u is the velocity at each point, and l is the position of finger, a free boundary whose velocity must consistently coincide with that of the fluid, u. This procedure not only allows us to handle a closed interface with an infinite $\partial_x h$ at the end point l, but it avoids the problem of supplying explicit boundary conditions to Eq. (12). This procedure includes the important physics of the droplet both in terms of shape and speed. In fact, in the absence of rotation, this resummation implies the relaxation to a circular interface. Moreover, in the presence of rotation it is known that an exact solution of the full Hele-Shaw equations is a circular droplet moving out of the rotation axis exponentially as discussed in [21]. The above resummation for the particular case of a free droplet would also tend asymptotically to that solution. Note that, even if the asymptotic solution is correct, it is not guaranteed in general that the dynamics outside the domain of validity of the lubrication approximation remains close to the exact one. In our case, however, a separation of time scales between the slow variable $l(t)$ and the fast relaxation of the interface shape in the droplet region ensures that the shape evolution is quasistatic.

Our fully implicit code simulates one quarter of the interface $(x>0,\ h>0)$ using initially $2N$ equidistant points at Δx where the different values of h_i are computed at the odd points of the mesh and u_i at the even. Boundary conditions at $x=0$ are $u(-x)=u(x)$ and $h(-x)=h(x)$. At $x=l$ we have $h=0$ and $u(l)$ is computed using the symmetry of the negative part $(x>0,\ h<0)$ of the interface. The error is controlled by a combination of the computations for time steps dt and $dt/2$, which yields corrections of order dt^3. We reject a time step when the relative error at any point in u and h (difference in the result between performing one dt step and two $dt/2$ steps) is larger than 5%. In this case, we proceed to reduce dt by half and try again until an optimum value of dt is reached. This control allows us to have an adaptive time step from the initial time step until the end of the simulation run.

As the interface evolves, a new mesh is generated when the condition that the number of mesh points between the points $x_{\min}$ and x_b [where $h(x_{\min})=H_{\min}$ and x_b is the point where $h(x_b)=2H_{\min}$] is larger than a certain fixed value N_m does not hold. Whenever this condition is not fulfilled the number of data points is increased and a new refined mesh with new values h and u is generated using interpolated data from the previous time step. This new mesh is constructed as follows. First, it has a smaller fixed $\delta x_s < \Delta x$ distance between points in the singular region (approximately symmetric around the minimum) providing the necessary accuracy in our simulations. As one moves away from the singular region the distance between the mesh points is progressively increased. This is accomplished multiplying the spatial step by the same factor α for each consecutive point until the original Δx is recovered. From then on, the spatial distance between the different points is again Δx.

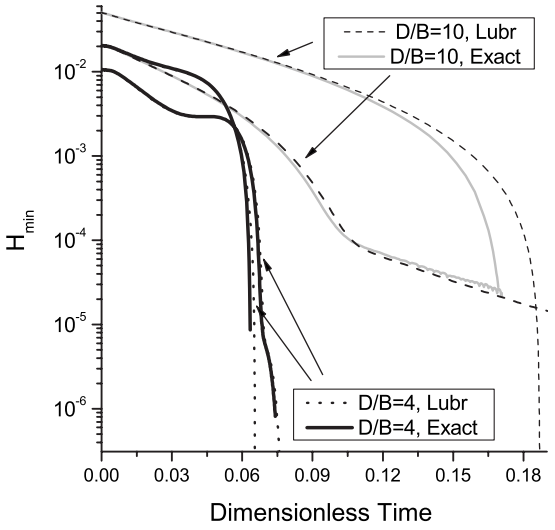

FIG. 3. The minimum value of the filament is compared for the lubrication approximation and the exact evolution in four different cases. Two runs with $D/B=4$ and two runs with $D/B=10$ using different initial conditions [different $H_{\min}(t=0)=H_0$].

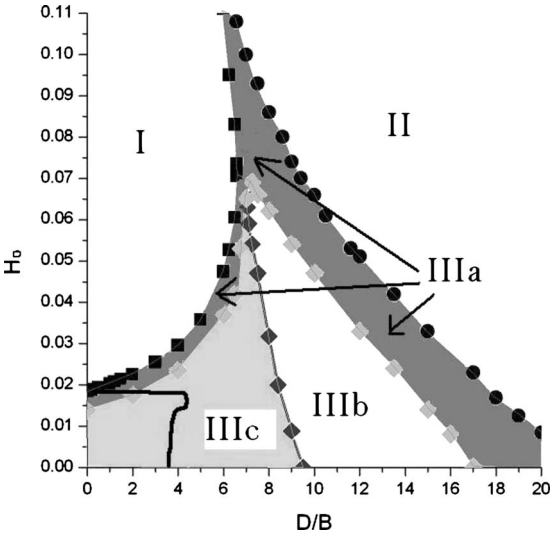

FIG. 4. Basin of attraction of five different attractors in the space generated by our uniparametric family of solutions (defined by H_0) and D/B. Region I is the basin of attraction of a centered stable droplet without pinch-off. Region II corresponds to a thin filament with a droplet at the top which reaches infinity. Regions IIIa, b, and c have in common that the minimum of the interface diminishes very rapidly at some moment of the evolution. The differences among them are explained in the text. Black dots and circles, together with gray diamonds, indicate the points where transitions among the different attractors have actually been computed. The thick line at the bottom left indicates the set of initial conditions for which the argument based on the nonuniform time rescaling (see Sec. V B) would predict also finite-time pinch-off in the presence of rotation.

We have changed N_m and α in our simulations to study its robustness and the time required to perform a typical simulation. Simulations are fairly insensitive to N_m as long as $N_m>10$. Increasing this value does not affect the results and only increases the time computation (at least for $N_m<50$). On the contrary simulations are more sensitive to α. It cannot be too small since it makes the simulations extremely time-consuming, nor very large since accuracy and eventually instabilities can appear. We take $\alpha=1.005-1.02$ as the appropriate range of intermediate value with robust results.

This numerical scheme based on the lubrication approximation which uses an adaptive mesh is much more efficient than the full Eqs. (1)–(3) which contain complex integrals. The latter scheme is time-consuming owing to stiffness and numerical instability, in particular for adaptive meshes. However, it is worth showing the explicit comparison of both numerical evolutions for times as long as possible, in particular because the conditions for the lubrication approximation are not fulfilled in the entire system (the droplet region), while the problem is strictly speaking nonlocal. To this purpose we have computed the exact evolution as defined at the beginning of Sec. II. We have removed the main part of the stiffness by treating the singular terms (those appearing in the lubrication approximation) implicitly. The limiting factors for this integration are stability and computation time.

In Fig. 3 we use two different rotation parameters $D/B=4$ and $D/B=10$. For each one we use two different initial conditions [different $H_{\min}(t=0)=H_0$]. All in all, four initial interfaces have been evolved using the exact and the lubrication approximation making a total of eight runs. Thick continuous lines represent evolutions using the full exact equations. Discontinuous thinner lines are evolutions using the lubrication approximation. We show that both exact and approximate solutions differ only slightly, both preserving the nontrivial transitions between different qualitative behaviors through several orders of magnitude. Only for large initial filament thickness and large rotations can we find some significant differences. The pinching singular behavior is thus expected to be correctly captured by the lubrication approximation.

V. NUMERICAL RESULTS

A. Asymptotic behaviors

Figure 4 shows the basins of attraction of the different asymptotic behaviors for the space of initial conditions of class (16) parametrized by $H_0=h(x=0,\ t=0)$, which is also the minimum of the interface $H_{\min}$ at $t=0$, as a function of the ratio D/B which measures the competition between centrifugal and capillary forces. The region marked as I includes the initial conditions for which capillary forces strongly dominate to the point that the interface evolves toward a centered stable drop around the axis of rotation (see top of Fig. 5). Region II on the right designates those initial conditions for which centrifugal forcing dominates. Those initial conditions evolve to form a thin filament which stretches exponentially with two drops at the end that escape also exponentially toward infinity (see bottom of Fig. 5). Within numerical accuracy, we must conclude that region II corresponds to (exponential) pinch-off at infinite time. Region III in between exhibits a more complex behavior owing to a subtle competition between capillary and centrifugal forces. Black squares (circles) indicate where the transition from

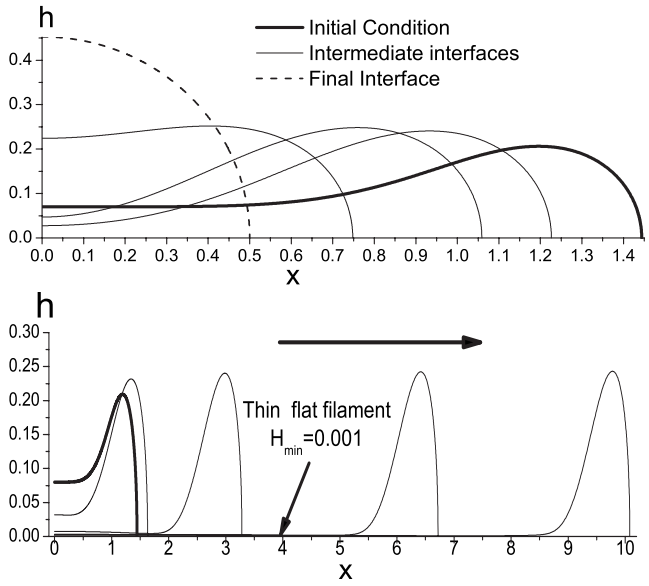

FIG. 5. Evolution of the global shape of the interfaces. Top: initial condition going to centered mass; corresponds to region I in Fig. 4. Bottom: example of region II where the initial condition goes to a drop reaching infinity without apparent finite-time pinch-off.

region I (region II) and III was found. Gray diamonds indicate the points where difference of behavior within region III was found. The location of all these points is accurate up to 10% (which is indicated roughly by the size of the symbol) when we changed the parameters α and N_m. Therefore, even the presence of the sliver of region IIIa is very robust to changes in mesh accuracy, if only slightly thinner or wider depending on the accuracy of the mesh.

All initial conditions in region III exhibit a sudden drop of $H_{\min}$ which becomes very small. The characteristic evolution of the interfaces in this region is depicted in Fig. 6. The apparent tendency to finite-time pinch-off is, in some cases, overcome by centrifugal forces. The line which separates regions IIIb and IIIc is also the limit between a droplet approaching the center of the cell (on the left) or a droplet evolving toward infinity (on the right). All cases marked as IIIa lead to finite-time pinch-off to within the achievable numerical accuracy [see Fig. 6 (middle) and Fig. 7]. Region IIIb includes those for which a very fast decay in $H_{\min}$ (which may lead one to think there is a pinch-off singularity) is overcome after a finite time by the centrifugal forcing, which reduces the decay to an exponential which persists for the simulation time [see Fig. 6 (bottom) and also Fig. 8].

Finally, initial conditions in region IIIc have in common the fact that the droplets are receding toward the center. The interface seems to approach pinch-off faster than exponential, but at some point this fast decay stops changing behavior and exhibiting in some cases nonmonotonic rebound. After this rebound the minimum of the interface starts decaying again in a rather smooth way which makes it difficult to conclude numerically whether the finite-time pinch-off will indeed occur. Figure 9 shows a series of evolution of the minimum point of the interface for $D/B=6$ and with different H_0 where such rebounds can be seen. The corresponding complete interface of one of those cases is at the top panel depicted in Fig. 6. It is clear from the final decay that the approach to pinch-off is faster than exponential but lower than the fast finite-time pinch-off observed in region IIIa in Fig. 7. The behavior in this region is basically the same reproduced by Almgren *et al.* [17,18] at $D/B=0$ (notice that at $D/B=0$ Fig. 4 shows that there is a part in region IIIa and another in region IIIc) but extended to cases where rotation is present.

To sum up, the differences between a, b, and c areas indicate whether this rapid decay produces a real finite-time pinch-off (IIIa), eventually changes behavior toward a slow but probable (though inconclusive) finite-time pinch-off near the center of the cell because the drop propagates inward (IIIc), or toward an infinite-time pinch-off after a very sharp decay close to the bubble propagating outward (IIIb).

It is worth remarking that the transitions between region IIIa and both IIIb and IIIc are numerically quite sharp. In fact, the thickness at which points in regions IIIb and IIIc show a change in behavior with time decreases abruptly by several orders of magnitude as we approach the boundary. We define the borderline at those points where we see no change in behavior within our numerical reach (10^{-16}). So even though we cannot rule out a change in behavior after that, the fact that this is moved so fast to extremely small values of thickness suggests that there is indeed a qualitative change in the asymptotics.

B. Effective boundary conditions

In Sec. III we discussed a mapping of the lubrication equation with rotation to the one without rotation. Accordingly, the only reason why the two problems are not equivalent up to a change of variables in the lubrication region is that the corresponding boundary conditions are not mutually transformed by the same mapping. The boundary conditions that need to be specified for the lubrication equation are defined by the matching conditions with the (nonlubricating) region defined by the rounded droplet closing the filament. Note that even for the local approximation [Eq. (17)] where higher orders have been included, transformation (14) does not leave the equations invariant. In this context it is interesting to discuss the actual boundary conditions that must be applied to the transformed problem in order to realize the observed behavior of the original one.

In Fig. 4, the region enclosed by the thick line on the bottom left defines the set of initial conditions for which the naive argument based on the nonuniform time rescaling would predict also finite-time pinch-off in the presence of rotation. This corresponds to the condition $D/B < 1/[5\tau_0(H_0)]$, where $\tau_0(H_0)$ is the time of pinch-off for $D/B=0$, as a function of the initial interface parametrized by H_0. In this region the time rescaling provides a reasonable approximation of the pinch-off time. Obviously, within this approximation, if there is no finite-time pinch-off (for an initial thickness $H_0>0.02$) without rotation ($D=0$), there cannot be for any D. Figure 4 clearly shows that this is not the case for very large regions where we find finite-time pinch-off. In other words, we find that the effective boundary

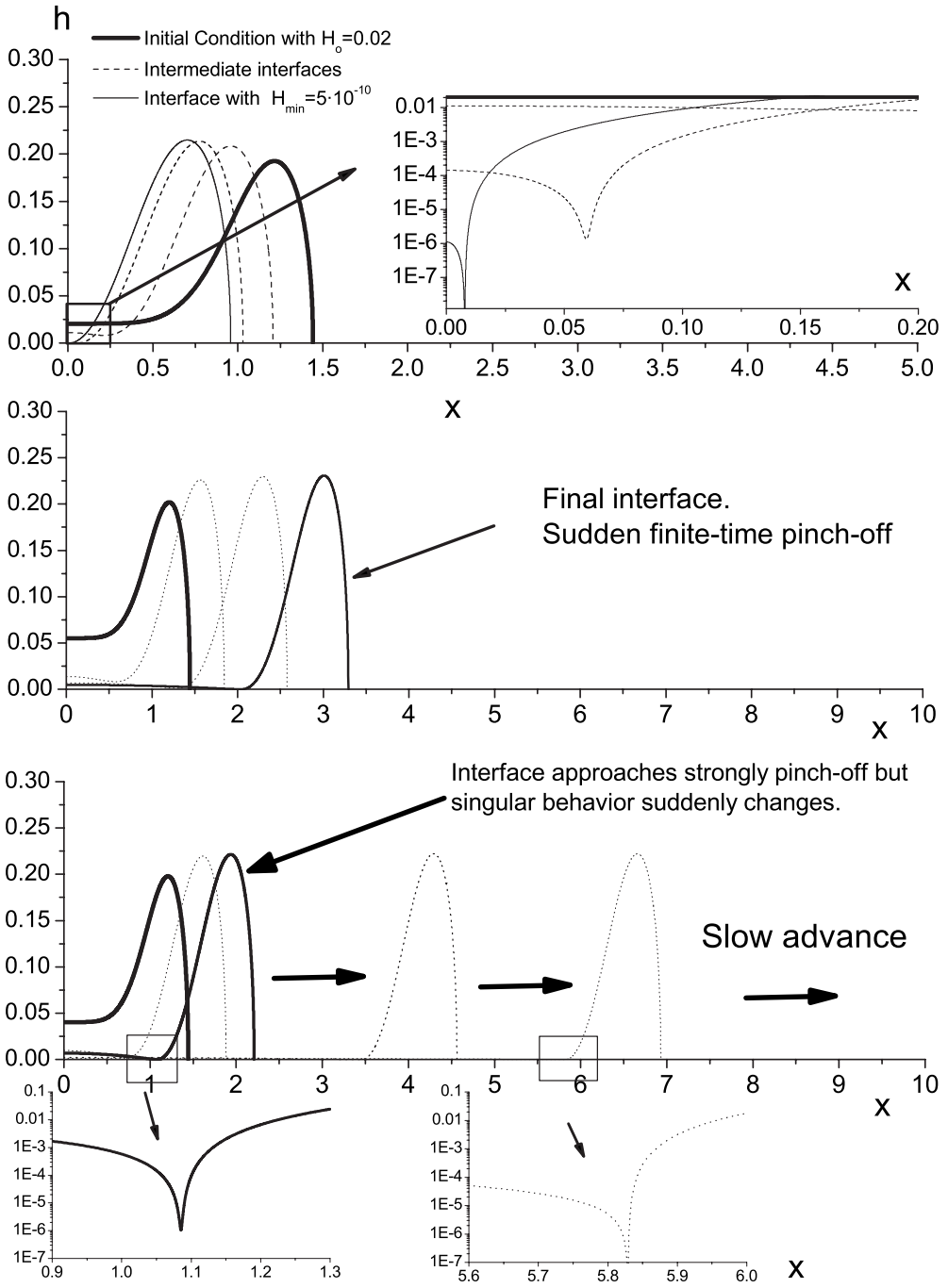

FIG. 6. Evolution of the global shape of the interfaces. Top: initial condition where the drops goes toward the center of the cell while the minimum decreases sharply (inset) and later rebounds slightly making finite-time pinch-off inconclusive (region IIIc). Middle: interface reaching finite-time pinch-off (region IIIa). Bottom: the drop evolves toward infinite and the minimum of the interface initially has a sharp decay but changes behavior suddenly toward infinite-time pinch-off (region IIIb) with the corresponding drop advancing but with a filament thickness which has reached extremely low values ($H_{\min}=10^{-8}$).

conditions on the lubrication approximation play a crucial and subtle role regarding the existence of finite-time singularities.

In order to visualize in more detail the role of the boundary conditions, in Fig. 10 we compare three different evolutions for two representative initial conditions which both lead to finite-time pinch-off with rotation. The solid curve is a snapshot of the evolution with rotation right before pinch-off. In the dashed line, we plot a snapshot of the evolution without rotation ($D=0$) at the corresponding time as given by time rescaling (14). Finally, as a dotted line we plot this last curve but now rescaled also in both x and h defined by the same mapping. This is the curve that would correspond to the case with rotation if the mapping were exact, including the boundary conditions. The large discrepancy between the solid and the dotted lines clearly reflects that the mapping is not exact for the whole problem but allows also to visualize how this discrepancy translates into the differences in the

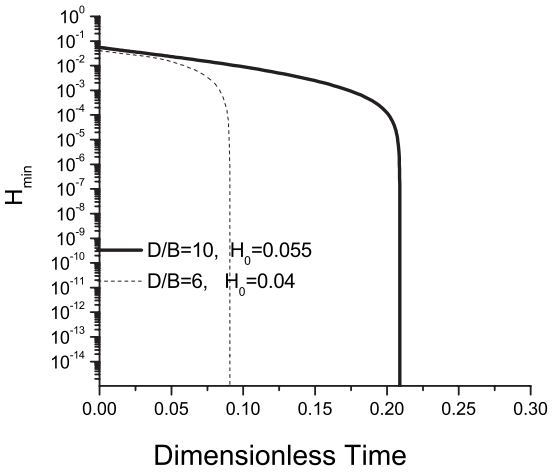

FIG. 7. The minimum of the interface as a function of dimensionless time for two different initial conditions inside area IIIa.

matching region between the filament and the droplet.

In the upper case of Fig. 10 the droplet is receding toward the center and the mapping would predict that there should be no finite-time pinch-off even though there could be one in the absence of rotation. In the lower case, the evolution without rotation would lead to an infinite stretching of the lubrication region without finite-time pinch-off, while again, the correct boundary condition does lead to finite-time pinch-off for the case with rotation.

VI. SUMMARY, DISCUSSION, AND CONCLUSION

In this paper we have derived the lubrication approximation for Hele-Shaw flows with centrifugal forcing for radial filaments. We have concentrated mostly on the case of high viscosity contrast for which the lubrication approximation is shown to be local. The lubrication analysis shows that, even though the rotation tends to create thin stretching filaments, the centrifugal forcing generally competes against capillary forces. In the case when capillary forces dominate over centrifugal forces, the behavior is an extension of previous results in Refs. [17,18].

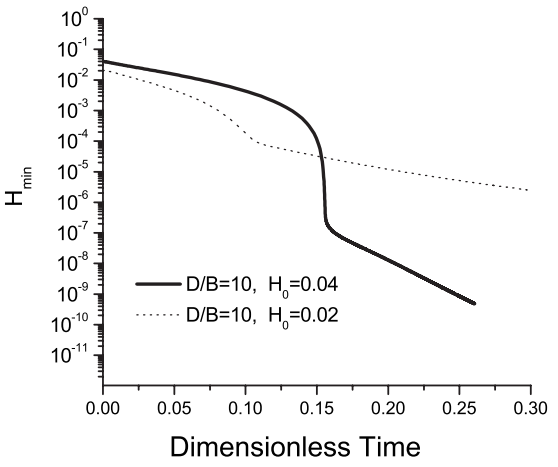

FIG. 8. The minimum of the interface as a function of dimensionless time for two different initial conditions inside area IIIb.

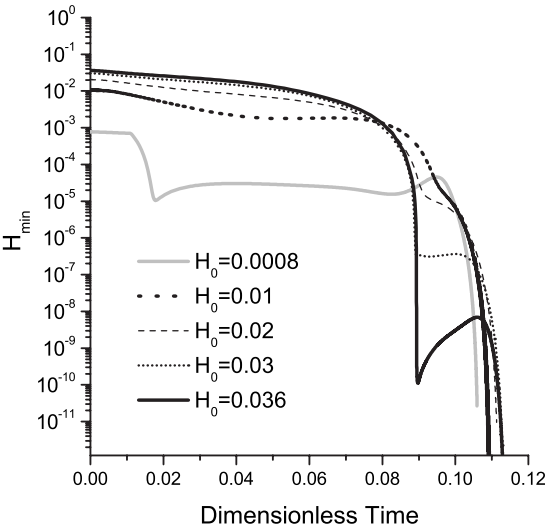

FIG. 9. The minimum of the interface as a function of dimensionless time for five initial conditions all of them using $D/B=6$ belonging to area IIIc.

We have shown that when the two competing forces are comparable, the phase space of possible asymptotic behavior is complex. We have obtained this phase space numerically in detail for the same class of initial conditions studied in [17,18]. Our focus has been the existence of finite-time singularities rather than in the characterization of their self-similar scaling, which remains an open question when rotation is present. In particular we have shown that the matching of the lubrication region to the droplet region end-

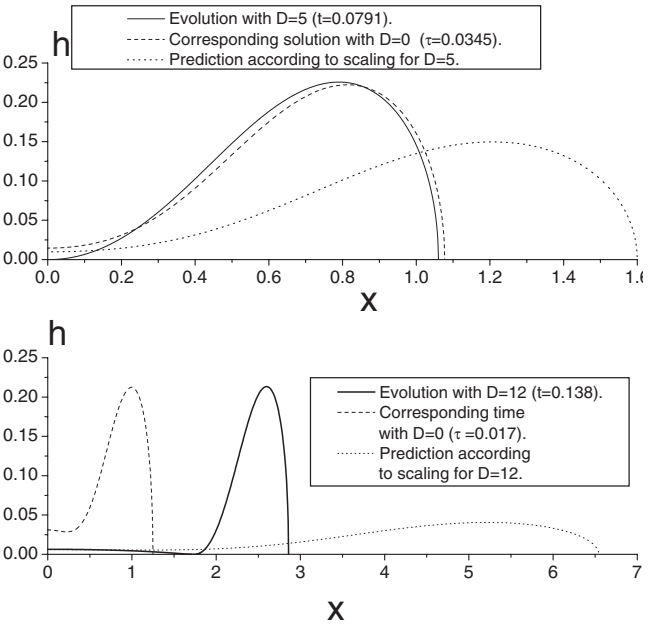

FIG. 10. Effect of boundary conditions imposed by the matching between the lubrication region and the droplet. The three interfaces in each plot represent the actual evolution with rotation up to the pinch-off time (black), the interface evolved without rotation with the correspondingly scaled time [dashed interface with $D=0$ at $\tau = \frac{B}{5D}(1-e^{-5Dt})$], and the latter with the scaling defined by Eq. (14) (dotted). See discussion in the text.

ing the finger yields a nontrivial boundary condition for the lubrication equation that plays a crucial role for the existence of finite-time singularities and gives rise to the complex nonlinear behavior of the intermediate region.

Finally, for the regime dominated by centrifugal forces, the present study confirms the experimental observation [19] and the numerical evidence [21], that, in the high viscosity-contrast limit ($A=1$), finite-time singularities do not occur. The fact that area II is relatively large explains both the experimental results of Ref. [19] and the phase-field simulations of Ref. [21]. For high rotation speeds $D/R>20$ the filament seems to approach infinity without pinch-off regardless the initial condition or initial thickness. These values of rotation are the typical ones reported in experiments up to now. This is in contrast to cases with $A<1$, which do exhibit frequent pinch-off even in the regime dominated by centrifugal forces [19,21].

While the question of the occurrence of pinch-off for low viscosity contrasts when centrifugal and capillary forces are comparable remains open, we can conclude that sufficiently fast rotation produces conditions with long, thin filaments of arbitrarily small thickness, but which do not pinch at finite time. This suggests that rotation could be used as a means to prepare initial conditions to study pinch-off of interfaces experimentally, in particular for the most common situation where only capillary forces drive the dynamics (by switching off the rotation). Comparison between experiments on the one hand and theory and numerical simulation on the other could shed light on the issue of the three-dimensional effects on real Hele-Shaw pinch-off events. Occurrences of pinch-off events in situations with good control of the initial conditions where the theory does not predict them could be traced back to three-dimensional effects and help establish the limitations of the effective two-dimensional description of Hele-Shaw flows. We have performed simulations of this possible scenario for different parameters in region II stopping the rotation when the interface reached a given length $l=10$. A typical result of this is shown in Fig. 11. After rotation is switched off the droplets start receding and the filament thickness decreases smoothly. Eventually, the droplet reaches the center of the cell. At this point the interface develops a finite-time pinch-off close to (but at a certain distance of) $x=0$.

We conclude by proposing an experiment based on these simulations. The basic idea is to look for early pinch-off in a region close to the droplet after the rotation is stopped. In the case where this pinch-off is present, it could only be attributed to three-dimensional effects of the cell. On the contrary, to the extent that such pinch-off events near the droplet are not taking place, one should conclude that the effective two-dimensional Hele-Shaw description is correct. Ultimately, such experiments could explore quantitatively the value and dependence on parameters and conditions (wetting properties of the cell, etc.) of the cutoff length that limits the validity of the 2D Hele-Shaw equations [21].

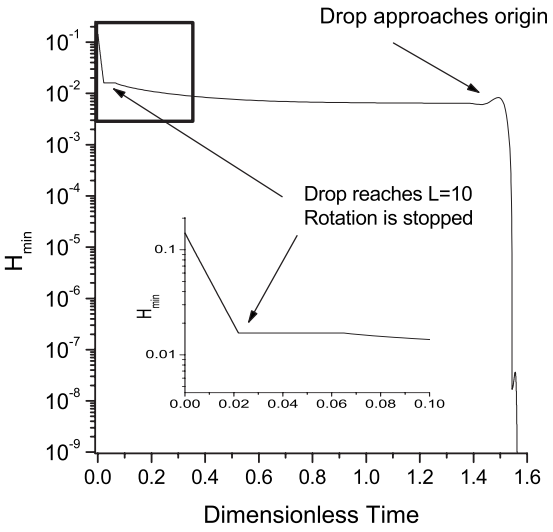

FIG. 11. Evolution of an interface at $D/B=100$ with $H_0=0.15$ Rotation is stopped when the droplet reaches $l=10$ (interface A in the bottom graph). The initial exponential decay stops when rotation is switched off (top graph) and the droplet starts receding toward the center of the cell (interface B) at the same time that the thickness of the filament decays slowly. Once the droplet reaches the center of the cell (interface C), this behavior changes abruptly reaching finite-time pinch-off.

ACKNOWLEDGMENTS

Financial support of Project No. FIS2006-03525 from Ministerio de Ciencia e Innovación (MICINN, Spain) is acknowledged. E.A.-L. also acknowledges a Juan de la Cierva grant from MICINN.

[1] J. Eggers, Rev. Mod. Phys. **69**, 865 (1997).
[2] M. Moseler and U. Landman, Science **289**, 1165 (2000).
[3] J. Eggers, Phys. Rev. Lett. **89**, 084502 (2002).
[4] A. Oron, S. H. Davis, and S. G. Bankoff, Rev. Mod. Phys. **69**, 931 (1997).
[5] G. Tryggvason and H. Aref, J. Fluid Mech. **154**, 287 (1985).
[6] D. Bensimon, L. P. Kadanoff, S. Liang, B. I. Schraiman, and C. Tang, Rev. Mod. Phys. **58**, 977 (1986).
[7] J. Casademunt, Chaos **14**, 809 (2004).
[8] L. Carrillo, F. X. Magdaleno, J. Casademunt, and J. Ortín, Phys. Rev. E **54**, 6260 (1996).
[9] E. Alvarez-Lacalle, J. Casademunt, and J. Ortín, Phys. Rev. E **64**, 016302 (2001).
[10] E. Alvarez-Lacalle, E. Pauné, J. Casademunt, and J. Ortín, Phys. Rev. E **68**, 026308 (2003).
[11] W. W. Zhang and J. R. Lister, Phys. Fluids **11**, 2454 (1999).
[12] R. E. Goldstein, A. I. Pesci, and M. J. Shelley, Phys. Rev. Lett. **70**, 3043 (1993).
[13] P. Constantin, T. F. Dupont, R. E. Goldstein, L. P. Kadanoff, M. J. Shelley, and S.-M. Zhou, Phys. Rev. E **47**, 4169 (1993).

[14] T. F. Dupont, R. E. Goldstein, L. P. Kadanoff, and S.-M. Zhou, Phys. Rev. E **47**, 4182 (1993).
[15] R. E. Goldstein, A. I. Pesci, and M. J. Shelley, Phys. Rev. Lett. **75**, 3665 (1995).
[16] R. E. Goldstein, A. I. Pesci, and M. J. Shelley, Phys. Fluids **10**, 2701 (1998).
[17] R. Almgren, Phys. Fluids **8**, 344 (1996).
[18] R. Almgren, A. Bertozzi, and M. Brenner, Phys. Fluids **8**, 1356 (1996).
[19] E. Alvarez-Lacalle, J. Casademunt, and J. Ortín, Phys. Fluids **16**, 908 (2004).
[20] E. Alvarez-Lacalle, J. Ortín, and J. Casademunt, Phys. Rev. E **74**, 025302(R) (2006).
[21] R. Folch, E. Alvarez-Lacalle, J. Ortín, and J. Casademunt, Phys. Rev. E **80**, 056305 (2009).
[22] J. Eggers and T. F. Dupont, J. Fluid Mech. **262**, 205 (1994).
[23] Note that the linear growth of the vorticity with x in Eq. (10e) produces an apparent divergence of the integrals in Eq. (7) if considered separately and taken all the way to infinity. Note, however, that these would be naturally regularized for a closed (finite) interface and the two integrals in Eq. (7) would cancel with each other the diverging part in the limit where the closure of the interface is taken to infinity.